maternal disomy of this region causes Prader-Willi syndrome (PWS). PWS is a neurobehavioral disorder characterized by hypotonia and respiratory distress in neonatal stage, and hyperphagia followed by severe obesity, hypogonadism, and behavioral problems in childhood. These complex symptoms are all thought to be due to hypothalamic deficiency.

Although the molecular mechanism is not clear, Necdin may be a candidate gene susceptible for PWS. Necdin-mutant mice have been generated by several independent groups and display different phenotypes likely due to differences in the targeting constructs or in the genetic backgrounds of the mice. For example, although Tsai and colleagues failed to detect neonatal lethality or infertility on their Necdin-mutant mouse line (60), Gerard and others reported early postnatal death in some paternally inherited Necdin-mutant mice (61). These newborn mice demonstrate abnormal neuronal activity within the putative respiratory-generating center (62). Neuronal abnormalities were also observed in the Necdin-mutant line generated by Muscatelli and colleagues. These mice also displayed neonatal lethality of variable penetrance depending on genetic backgrounds. Mice that survived show some behavioral alterations, such as increased skin scraping, and a reduced number of neurons producing hypothalamic oxytocin and lutenizing hormone-releasing hormone (LH-RH) (63). Aspects of the phenotype observed in this Necdin-mutant strain are reminiscent of defects observed in human PWS.

One explanation for the variable phenotypes seen in Necdin-mutant mice (60,61,63) is that the targeting constructs may influence the expression level of nearby genes. Although three of the maternally imprinted genes (SNRPN, IPW, or ZNF127) residing in the region near NDN have been disrupted with no obvious phenotype (59), the possibility has not been excluded that these genes may contribute to defects observed in PWS when lost in combination with Necdin. Another gene in the MAGE superfamily is MAGEL2/NDNL1. It shares 51% amino acid sequence similarity to Necdin and is located 41 kb distal to NDN in the PWS imprinting lesion (64). MAGEL2/NDNL1 is also expressed in developing neuronal tissue including the hypothalamic region. Because a knockout of this gene has not yet been published, the significance of MAGEL2/NDNL1 on pathogenesis of PWS is still unknown.

Most MAGE genes are encoded on the X chromosome, and of the few remaining genes located on autosomes, Necdin and MAGEL2 are imprinted. It is widely accepted that one of the two female X chromosomes is silenced to equalize X-linked gene dosage between XX and XY individuals. Genomic imprinting and X chromosome inactivation share some similarity in molecular mechanisms. Because it is thought that imprinting is first fixed on the X chromosome and subsequently acquired by autosomes (65), it is intriguing that NDN and MAGE-L2 may, in the course of MAGE gene duplication and chromosomal translocation, choose an imprinted locus in the autosome.

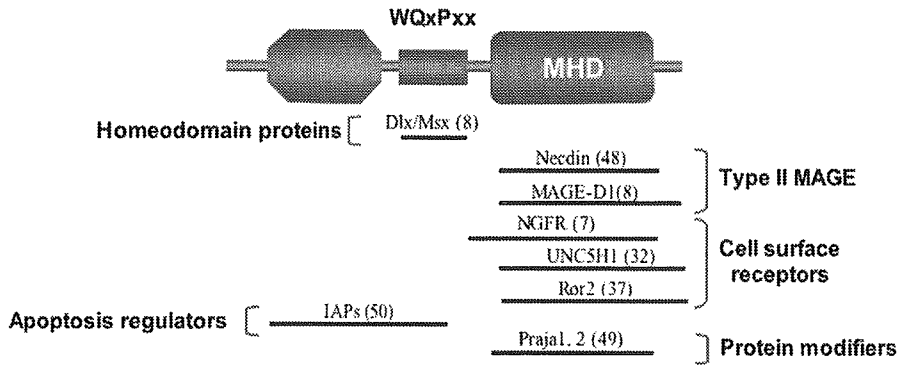

Figure 3: MAGE-D1-interacting proteins. Putative binding domains are shown. See details in the text.

Still Open Questions

We have described roles for MAGE-D1 that have been suggested by the identification and analysis of a number of associated molecules (Fig. 3). Because interactors of MAGE-D1 include cell surface receptors, transcription factors, intracellular effectors of apoptosis and protein modifiers, we may regard MAGE-D1 as a new adaptor protein with various functions in intracellular signaling. It is noteworthy that MAGE-D1 may be downstream of a number of apoptotic pathways, each caused by distinct input signals, namely, p75NTR-dependent apoptosis, UNC5H-dependent apoptosis, and possibly BMP-dependent apoptosis. Furthermore, by interacting with IAPs, MAGE-D1 also regulates the caspase activity downstream of these apoptotic pathways.

MAGE-D1 shares some binding partners with other type II MAGE proteins. For example, p75NTR also binds to MAGE-G1, MAGE-H1, and Necdin; and Praja1 also binds Necdin. Interactions suggest there may be functional redundancy or antagonism among MAGE family proteins (49,57,66). These functional interactions may be due to the close homology observed in the MHD of MAGE family proteins. Interactions between family members via their MHD domains may also facilitate their association with other proteins. This occurs when MAGE-D1 binds Necdin and acts as an adaptor for Msx2 binding (48). Although these protein associations are central to the role this family of proteins plays in signal transduction, the precise mechanisms, specifically how the protein complexes associate or dissociate, remain to be clarified. Moreover, as in many cases of signal transduction, posttranslation modifications, such as ubiquitination, phosphorylation, acetylation, or proteolytic cleavage of the MAGE-D proteins, may be mechanisms that regulate their ability to interact with target molecules, but much remains to be learned about such mechanisms.

By now, our current knowledge about MAGE-D1 function is entirely dependent on in vitro functional approaches, because the in vivo data on the

physiological function of MAGE-D1 are still lacking. To date, several groups have succeeded in generating knockout mice for MAGE-D family genes, although no reports describing their phenotype have been published yet. This may be due to the fact that MAGE-D1 null mice appear to have partially penetrant phenotypes with some animals appearing normal (unpublished data). Thus, in contrast to the in vitro functional data, which suggest important roles for MAGE-D1 during neuronal and skeletal development, the in vivo data suggest that MAGE-D1 may be dispensable. A possible explanation for the lack of clear phenotype is that there may be functional redundancy among family members. In this case, generating a multigene knockout might be required, but it may be difficult to generate them by intercross of the knockout lines because all the MAGE-D genes are closely located on the X chromosome. Consequently, this analysis may require the advanced techniques like Cre-loxP systems to create knockout mice for multiple MAGE-D genes. Other animal models carrying single MAGE gene, such as *Drosophila* (9) and Zebrafish (10), may also contribute to clarifying the central role of MAGE proteins.

Although studies of MAGE-D1 and Necdin have given insight into the function of other MAGE proteins, these studies serve as only a starting point for uncovering the truth about MAGE proteins. A key to understanding the role of MAGE-D and other type II MAGE proteins will be to analyze the knockout phenotypes. These analyses, together with accumulating in vitro data defining binding partners and signaling pathways, will reveal how MAGE proteins contribute to development and disease.

ACKNOWLEDGMENTS

Authors (AS and KW) thank Drs. Yoshiko Masuda and Kyoji Ikeda for contribution in the series of our study on MAGE-D1. This work was supported in part by grant NS39572 from the NIH (to LH) and a grant for the Program for Promotion of Fundamental Studies in Health Sciences of the Organization for Pharmaceutical Safety and Research of Japan (to KW).

REFERENCES

1. van der Bruggen P, Traversari C, Chomez P, Lurquin C, De Plaen E, Van den Eynde B, Knuth A, Boon T. A gene encoding an antigen recognized by cytolytic T lymphocytes on a human melanoma. Science **1991**, *254*, 1643–1647.

2. Chomez P, De Backer O, Bertrand M, De Plaen E, Boon T, Lucas S. An overview of the MAGE gene family with the identification of all human members of the family. Cancer Res **2001**, *61*, 5544–5551.

3. Barker PA, Salehi A. The MAGE proteins: Emerging roles in cell cycle progression, apoptosis, and neurogenetic disease. J Neurosci Res **2002**, *67*, 705–712.

4. De Smet C, Lurquin C, Lethe B, Martelange V, Boon T. DNA methylation is the primary silencing mechanism for a set of germ line- and tumor-specific genes with a CpG-rich promoter. Mol Cell Biol **1999**, *19*, 7327–7335.

5. Boon T, Cerottini JC, Van den Eyende B, Van den Bruggen P, Van Pel A. Tumor antigens recognized by T lymphocytes. Annu Rev Immunol **1994**, *12*, 337–365.

6. Pold M, Zhou J, Chen GL, Hall JM, Vescio RA, Berenson JR. Identification of a new, unorthodox member of the MAGE gene family. Genomics **1999**, *59*, 161–167.

7. Salehi AH, Roux PP, Kubu CJ, Zeindler C, Bhakar A, Tannis LL, Verdi JM, Barker PA. NRAGE, a novel MAGE protein, interacts with the p75 neurotrophin receptor and facilitates nerve growth factor-dependent apoptosis. Neuron **2000**, *27*, 279–288.

8. Masuda Y, Sasaki A, Shibuya H, Ueno N, Ikeda K, Watanabe K. Dlxin-1, a novel protein that binds Dlx5 and regulates its transcriptional function. J Biol Chem **2001**, *276*, 5331–5338.

9. Pold A, Ma HJ, Sjak-Shieb NN, Vescio RA, Berensonb JR, Pold M. Identification of a new, unorthodox member of the MAGE gene family. Dev Comp Immunol **2000**, *24*, 719–731.

10. Bischof J, Ekker M, Wevrick R. A MAGE/NDN-like gene in zebrafish. Dev Dyn **2003**, *228*, 475–479.

11. Bertrand M, Huijbers I, Chomez P, Backer O. Comparative expression analysis of the MAGED genes during embryogenesis and brain development. Dev Dyn **2004**, *230*, 325–334.

12. Saburi S, Nadano D, Akama TO, Hirama K, Yamanouchi K, Naito K, Tojo H, Tachi C, Fukuda MN. The trophinin gene encodes a novel group of MAGE proteins, magphinins, and regulates cell proliferation during gametogenesis in the mouse. J Biol Chem **2001**, *276*, 49378–49389.

13. Sasaki M, Nakahira K, Kawano Y, Katakura H, Yoshimine T, Shimizu K, Kim SU, Ikenaka K. MAGE-E1, a new member of the melanoma-associated antigen gene family and its expression in human glioma. Cancer Res **2001**, *61*, 4809–4814.

14. Fukuda MN, Sato T, Nakayama J, Klier G, Mikami M, Aoki D, Nozawa S. Trophinin and tastin, a novel cell adhesion molecule complex with potential involvement in embryo implantation. Genes Dev **1995**, *9*, 1199–1210.

15. Albrecht DE, Froehner SC. DAMAGE, a novel alpha-dystrobrevin-associated MAGE protein in dystrophin complexes. J Biol Chem **2004**, *279*, 7014–703.

16. Stone B, Schummer M, Paley PJ, Crawford M, Ford M, Urban N, Nelson BH. MAGE-F1, a novel ubiquitously expressed member of the MAGE superfamily. Gene **2001**, *267*, 173–182.

17. Andrade MA, Perez-Iratxeta C, Ponting CP. Protein repeats: Structures, functions, and evolution. J Struct Biol **2001**, *134*, 117–131.

18. Brookfield JF. Genome sequencing: The ripping yarn of the frozen genome. Curr Biol **2003**, *13*, R552–R553.

19. Barker P. p75NTR is positively promiscuous: Novel partners and new insights. Neuron **2004**, *42*, 529–533.

20. Bibel M, Barde YA. Neurotrophins: Key regulators of cell fate and cell shape in the vertebrate nervous system. Genes Dev **2000**, *14*, 2919–2937.

21. Lee R, Kermani P, Teng K, Hempstead B. Regulation of cell survival by secreted proneurotrophins. Science **2001**, *294*, 1945–1948.

22. Beattie MS, Harrington AW, Lee R, Kim JY, Boyce SL, Longo FM, Bresnahan JC, Hempstead BL, Yoon SO. ProNGF induces p75-mediated death of oligodendrocytes following spinal cord injury. Neuron **2002**, *36*, 375–386.

23. Lu B. Pro-region of neurotrophins: Role in synaptic modulation. Neuron **2003**, *9*, 735–738.

24. Salehi AH, Xanthoudakis S, Barker PA. NRAGE, a p75 neurotrophin receptor-interacting protein, induces caspase activation and cell death through a JNK-dependent mitochondrial pathway. J Biol Chem **2002**, *277*, 48043–48050.

25. Bronfman FC, Tcherpakov M, Jovin TM, Fainzilber M. Ligand-induced internalization of the p75 neurotrophin receptor: A slow route to the signaling endosome. J Neurosci **2003**, *23*, 3209–3220.

26. Nielsen MS, Madsen P, Christensen EI, Nykjaer A, Gliemann J, Kasper D, Pohlmann R, Petersen CM. The sortilin cytoplasmic tail conveys Golgi-endosome transport and binds the VHS domain of the GGA2 sorting protein. EMBO J **2001**, *20*, 2180–2190.

27. Nykjaer A, Lee R, Teng K, Jansen P, Madsen P, Nielsen MS, Jacobsen C, Kliemannel M, Schwarz E, Willnow TE, Hempstead BL, Peterson CM. Sortilin is essential for proNGF-induced neuronal cell death. Nature **2004**, *427*, 843–848

28. Wang KC, Kim JA, Sivasankaran R, Segal R, He Z. P75 interacts with the Nogo receptor as a co-receptor for Nogo, MAG and OMgp. Nature **2002**, *420*, 74–78.

29. Mi S, Lee X, Shao Z, Thill G, Ji B, Relton J, Levesque M, Allaire N, Perrin S, Sands B, Crowell T, Cate RL, McCoy JM, Pepinsky RB. LINGO-1 is a component of the Nogo-66 receptor/p75 signaling complex. Nat Neurosci **2004**, *7*, 221–228.

30. Yamashita T, Tohyama M. The p75 receptor acts as a displacement factor that releases Rho from Rho-GDI. Nat Neurosci **2003**, *6*, 461–467

31. Kendall S, Goldhawk D, Kubu C, Barker P, Verdi J. Expression analysis of a novel p75(NTR) signaling protein, which regulates cell cycle progression and apoptosis. Mech Dev **2002**, *117*, 187–200.

32. Williams ME, Strickland P, Watanabe K, Hinck L. UNC5H1 induces apoptosis via its juxtamembrane region through an interaction with NRAGE. J Biol Chem **2003**, *278*, 17483–17490.

33. Hong K, Hinck L, Nishiyama M, Poo M, Tessier-Lavigne M, Stein E. A ligand-gated association between cytoplasmic domains of UNC5 and DCC family receptors converts netrin-induced growth cone attraction to repulsion. Cell **1999**, *97*, 927–941.

34. Llambi F, Causeret F, Bloch-Gallego E, Mehlen P. Netrin-1 acts as a survival factor via its receptors UNC5H and DCC. EMBO J **2001**, *20*, 2715–2722.

35. Tanikawa C, Matsuda K, Fukuda S, Nakamura Y, Arakawa H. p53RDL1 regulates p53-dependent apoptosis. Nat Cell Biol **2003**, *5*, 216–223.

36. Kanning KC, Hudson M, Amieux PS, Wiley JC, Bothwell M, Schecterson LC. Proteolytic processing of the p75 neurotrophin receptor and two homologs generates C-terminal fragments with signaling capability. J Neurosci **2003**, *23*, 5425–5436.

37. Matsuda T, Suzuki H, Oishi I, Kani S, Kuroda Y, Komori T, Sasaki A, Watanabe K, Minami Y. The receptor tyrosine kinase Ror2 associates with the melanoma-associated antigen (MAGE) family protein Dlxin-1 and regulates its intracellular distribution. J Biol Chem **2003**, *278*, 29057–290.

38. Ryoo H, Hoffmann H, Beumer T, et al. Stage-specific expression of Dlx-5 during osteoblast differentiation: Involvement in regulation of osteocalcin gene expression. Mol Endocrinol **1997**, *11*, 1681–1694.

39. Lee M, Kim YJ, Kim HJ, Park HD, Kang AR, Kyung HM, Sung JH, Wozney JM, Kim HJ, Ryoo HM. BMP-2-induced Runx2 expression is mediated by Dlx5, and TGF-beta 1

opposes the BMP-2-induced osteoblast differentiation by suppression of Dlx5 expression. J Biol Chem **2003**, *278*, 34387–34394.

40. Acampora D, Merlo GR, Paleari L, Zerega B, Postiglione MP, Mantero S, Bober E, Barbieri O, Simeone A, Levi G. Craniofacial, vestibular and bone defects in mice lacking the Distal-less-related gene Dlx5. Development **1999**, *126*, 3795–3809.

41. Depew MJ, Liu JK, Long JE, Presley R, Meneses JJ, Pedersen RA, Rubenstein JL. Dlx5 regulates regional development of the branchial arches and sensory capsules. Development **1999**, *126*, 3831–3846.

42. Zou H, Niswander L. Requirement for BMP signaling in interdigital apoptosis and scale formation. Science **1996**, *272*, 738–741.

43. Graham A, Francis-West P, Brickell P, Lumsden A. The signalling molecule BMP4 mediates apoptosis in the rhombencephalic neural crest. Nature **1994**, *372*, 684–686.

44. Yoda A, Oishi I, Minami Y. Expression and function of the Ror-family receptor tyrosine kinases during development: Lessons from genetic analyses of nematodes, mice, and humans. J Recept Signal Transduct Res **2003**, *23*, 1–15.

45. Patton M, Afzal A. Robinow syndrome. J Med Genet **2002**, *39*, 305–310.

46. Hikasa H, Shibata M, Hiratani I, Taira M. The Xenopus receptor tyrosine kinase Xror2 modulates morphogenetic movements of the axial mesoderm and neuroectoderm via Wnt signaling. Development **2002**, *29*, 5227–5239.

47. Brunelli S, Tagliafico E, De Angelis FG, Tonlorenzi R, Baesso S, Ferrari S, Niinobe M, Yoshikawa K, Schwartz RJ, Bozzoni I, Ferrari S, Cossu G. Msx2 and necdin combined activities are required for smooth muscle differentiation in mesoangioblast stem cells. Circ Res **2004**, *94*, 1571–1578.

48. Kuwajima T, Taniura H, Nishimura I, Yoshikawa K. Necdin interacts with the Msx2 homeodomain protein via MAGE-D1 to promote myogenic differentiation of C2C12 cells. J Biol Chem **2004**, *279*, 40484–40493.

49. Sasaki A, Masuda Y, Iwai K, Ikeda K, Watanabe K. A RING finger protein Praja1 regulates Dlx5-dependent transcription through its ubiquitin ligase activity for the Dlx/Msx-interacting MAGE/Necdin family protein, Dlxin-1. J Biol Chem **2002**, *277*, 22541–22546.

50. Jordan BW, Dinev D, LeMellay V, Troppmair J, Goetz R, Wixler L, Sendtner M, Ludwig S, Rapp UR. Neurotrophin receptor-interacting mage homologue is an inducible inhibitor of apoptosis protein-interacting protein that augments cell death. J Biol Chem **2001**, *276*, 39985–39989.

51. Liston P, Fong WG, Korneluk G. The inhibitors of apoptosis: There is more to life than Bcl2. Oncogene **2003**, *22*, 8568–8580.

52. Wen CJ, Xue B, Qin WX, Yu M, Zhang MY, Zhao DH, Gao X, Gu JR, Li CJ. HNRAGE, a human neurotrophin receptor interacting MAGE homologue, regulates p53 transcriptional activity and inhibits cell proliferation. FEBS Lett **2004**, *564*, 171–176.

53. Bruno T, De Angelis R, De Nicola F, Barbato C, Di Padova M, Corbi N, Libri V, Benassi B, Mattei E, Chersi A, Soddu S, Floridi A, Passananti C, Fanciulli M. Che-1 affects cell growth by interfering with the recruitment of HDAC1 by Rb. Cancer Cell **2002**, *2*, 387–399.

54. Taniura H, Taniguchi N, Hara M, Yoshikawa K. Necdin, a postmitotic neuron-specific growth suppressor, interacts with viral transforming proteins and cellular transcription factor E2F1. J Biol Chem **1998**, *273*, 720–728.

55. Taniura H, Matsumoto K, Yoshikawa K. Physical and functional interactions of neuronal growth suppressor necdin with p53. J Biol Chem **1999**, *274*, 16242–16248.

56. Taniguchi N, Taniura H, Niinobe M, Takayama C, Tominaga-Yoshino K, Ogura A, Yoshikawa K. The postmitotic growth suppressor necdin interacts with a calcium-binding protein (NEFA) in neuronal cytoplasm. J Biol Chem **2000**, *275*, 31674–31681.

57. Kuwako K, Taniura H, Yoshikawa K. Necdin-related MAGE proteins differentially interact with the E2F1 transcription factor and the p75 neurotrophin receptor. J Biol Chem **2004**, *279*, 1703–1712.

58. Uetsuki T, Takagi K, Sugiura H, Yoshikawa K. Structure and expression of the mouse necdin gene. Identification of a postmitotic neuron-restrictive core promoter. J Biol Chem **1996**, *271*, 918–924.

59. Yang T, Adamson T, Resnick J, Leff S, Wevrick R, Francke U, Jenkins NA, Copeland NG, Brannan CI. A mouse model for Prader-Willi syndrome imprinting-centre mutations. Nat Genet **1998**, *19*, 25–31.

60. Tsai T, Armstrong D, Beaudet A. Necdin-deficient mice do not show lethality or the obesity and infertility of Prader-Willi syndrome. Nat Genet **1999**, *22*, 15–6.

61. Gerard M, Hernandez L, Wevrick R, Stewart CL. Disruption of the mouse necdin gene results in early post-natal lethality. Nat Genet **1999**, *23*, 199–202.

62. Ren J, Lee S, Pagliardini S, Gerard M, Stewart CL, Greer JJ, Wevrick R. Absence of Ndn, encoding the Prader-Willi syndrome-deleted gene necdin, results in congenital deficiency of central respiratory drive in neonatal mice. J Neurosci **2003**, *23*, 1569–1573.

63. Muscatelli F, Abrous DN, Massacrier A, Boccaccio I, Le Moal M, Cau P, Cremer H. Disruption of the mouse necdin gene results in hypothalamic and behavioral alterations reminiscent of the human Prader-Willi syndrome. Hum Mol Genet **2000**, *9*, 3101–3110.

64. Lee S, Kozlov S, Hernandez L, Chamberlain SJ, Brannnan CI, Stewart CL, Wevrick R. Expression and imprinting of MAGEL2 suggest a role in Prader-Willi syndrome and the homologous murine imprinting phenotype. Hum Mol Genet **2000**, *9*, 1813–1819.

65. Lee J. Molecular links between X-inactivation and autosomal imprinting: X-inactivation as a driving force for the evolution of imprinting? Curr Biol **2003**, *13*, R242–54.

66. Tcherpakov M, Bronfman FC, Conticello SG, Vaskovsky A, Levy Z, Niinobe M, Yoshikawa K, Arenas E, Fainzilber M. The p75 neurotrophin receptor interacts with multiple MAGE proteins. J Biol Chem **2002**, *277*, 49101–49104.

Journal of Receptors and Signal Transduction, 25:199–216, 2005

ISSN: 1079-9893 print / 1532-4281 online
DOI: 10.1080/10799890500240781

Taylor & Francis
Taylor & Francis Group

A RANKL-Inducible Gene *Znf216* in Osteoclast Differentiation

Akinori Hishiya, Kyoji Ikeda, and Ken Watanabe

Department of Bone and Joint Disease, National Center for Geriatrics and Gerontology (NCGG), Obu, Aichi, Japan

Osteoclasts possess catabolic activity in mineralized tissues and are involved in bone remodeling coordinating with osteoblasts. Although the pathway using receptor and activator of NF-κB (RANK) and its ligand, RANKL, is known to be essential for osteoclast differentiation, their precise mechanisms are not fully understood. Using DNA microarray technology, we searched for genes that were up-regulated after RANKL stimulation in the macrophage cell line, RAW264.7 cells. A gene, *Znf216*, which encodes a zinc-finger protein, was detected among those genes up-regulated after RANKL stimulation. Expression of *Znf216* was also induced by other cytokines such as TNFα and IL-1β. Although ectopic expression of full-length ZNF216 abrogated osteoclast differentiation, its truncated forms accelerated it. No significant inhibitory effect on the NF-κB pathway was observed, however. These results suggest that ZNF216 is a potent inhibitory factor for osteoclast differentiation and that the mechanism is unlikely due to direct attenuation of the NF-κB pathway.

Key Words: RANKL; cDNA microarray; ZNF216

INTRODUCTION

Osteoclasts are multinucleated giant cells derived from the hematopoietic lineage (1). A number of extracellular factors expressed at distinct stages are involved in osteoclast differentiation (2,3). For example, studies in the *op / op* mice, which are severely osteopetorotic due to the absence of osteoclasts, revealed that M-CSF plays a critical role in osteoclast differentiation (4). Proinflammatory cytokines, such as TNFα and IL-1β also accelerate osteoclast differentiation (5,6).

Address correspondence to Ken Watanabe, PhD, Department of Bone and Joint Disease, National Center for Geriatrics and Gerontology (NCGG), 36-3 Gengo, Morioka-cho, Obu, Aichi 474-8522, Japan. Tel: +81-562-46-2311; Fax: +81-562-44-6595; E-mail: kwatanab@nils.go.jp

Among the cytokines, the essential key regulator for osteoclast differentiation is a TNF family cytokine, RANKL (7,8). Mice lacking RANKL or its receptor, RANK, display severe osteopetorosis with a complete absence of osteoclasts, suggesting that the RANKL-RANK pathway is indispensable for osteoclast differentiation (9,10). This pathway promotes not only osteoclast differentiation but also activation (7) and survival (11).

The intracellular signaling events that mediate osteoclast differentiation have been studied by using genetic approaches. Double knockout mice of the p50 and p52 subunits of the transcription factor, NF-κB, display osteopetrosis as seen in RANKL null mice (12). NF-κB functions downstream of the RANKL-RANK pathway and presumably activates genes necessary for osteoclast differentiation. Knockout mice for *fos*, a member of the AP-1 family, also exhibit osteopetorosis (13). c-Fos is thought to be activated by the RANKL-RANK pathway, although the precise mechanism of action remains unknown (14). In addition, src kinase is activated by the RANKL-RANK pathway, and even though src-deficient mice display normal number of osteoclasts, their resorption activity is impaired (15,16). Src is known to be localized to ruffled border membranes, where bone resorption takes place (17). Collectively, these results show that a number of signaling molecules are involved in RANKL-induced osteoclast differentiation and function, although the downstream and the regulatory mechanism have not been fully elucidated.

In the present study, we used cDNA microarray technology to elucidate changes in gene expression during osteoclast differentiation. Among the genes up-regulated, *znf216* is also activated by proinflammatory cytokines, such as TNFα and IL-1β. Furthermore, overexpression of ZNF216 strongly inhibits RANKL-induced osteoclast differentiation. Thus, novel negative regulation may exist for osteoclast differentiation downstream of RANKL stimulation.

MATERIALS AND METHODS

Antibodies and Reagents

Anti-ZNF216 antibody was raised against a synthesized peptide corresponding to the C-terminal sequence of mouse ZNF216 (amino acids 200–213). Mouse monoclonal antibodies for FLAG (M2 and M5) and tubulin (B-5-1-2) were purchased from Sigma (St. Louis, MO, USA). Antibodies against IκBα (C-21), p50 (C-19), p52 (C-5), and p65 (A) were obtained from Santa Cruz Biotechnology (Santa Cruz, CA, USA). RANKL, TNFα, and IL-1β were purchased from R&D Systems (Minneapolis, MN, USA). Lipopolysaccharide (LPS) and TPA (12-*O*-tetradecanoylphorbol-13-acetate) were purchased from Sigma and IFNγ from Genzyme (Cambridge, MA, USA).

Cell Culture Transfection

RAW264.7 mouse monocyte/macrophage cells were maintained in α-modified Eagle's medium (αMEM) containing 10% heat-inactivated fetal bovine serum (FBS) supplemented with penicillin, streptomycin, and L-glutamate. For in vitro osteoclastogenesis, RAW264.7 cells were plated at a density of $1.3 \times 10^4/cm^2$ and incubated overnight. Recombinant mouse RANKL was then added to a final concentration of 10 ng/mL. To detect tartrate-resistant acid phosphatase (TRAP) activity, a hallmark of osteoclasts, cells were fixed with an acetone-citrate-formalin solution (65:27:7) and stained by using a leukocyte acid phosphatase kit (Sigma Diagnostics). For isolation of RNA, RAW264.7 cells were stimulated with TNFα (10 ng/mL), IL-1β (10 ng/mL), LPS (10 μg/mL), TPA (1 mM), or IFNγ (100 U/mL), and harvested at the indicated time points. RANK293 cells, which constitutively express RANK, were kindly provided by Drs. Naoki Sakurai (Tanabe Seiyaku Co., Ltd., Osaka, Japan) and Kunihiro Matsumoto (Nagoya University, Japan) (18). HEK293 and RANK293 cells were cultured at 37°C in Dulbecco's modified Eagle's medium (DMEM) containing 10% heat-inactivated FBS supplemented with penicillin and streptomycin. FuGENE6 (Roche Diagnostics, Mannheim, Germany) was used for transfection. RAW264.7 cells stably expressing full-length or truncated forms of ZNF216 were established by infection using Pantropic Retroviral Expression System (Clontech Laboratories, Palo Alto, CA, USA) and maintained in media containing puromycin.

Isolation of RNA and cDNA Microarray

Total RNA was isolated from RAW264.7 cells at 24, 48, and 72 hr after addition of RANKL. Untreated RAW264.7 cells were used as $t = 0$ hr control. Total RNA was purified by using TRIZOL Reagent (Invitrogen, Carlsbad, CA, USA), according to the manufacturer's instructions. Purification of mRNA was performed by using Micro-Fast Track 2.0 (Invitrogen). Purified mRNA was subsequently used for cDNA microarray analyses (Mouse GEM-I, Incyte Genomics, Palo Alto, CA, USA).

Plasmid Construction

Full-length ZNF216 cDNA was amplified by reverse transcription-coupled PCR (RT-PCR) and subcloned into pBabe-puro retrovirus vector or pEF4 /Myc-HisA (Invitrogen) with a FLAG epitope tag at the N-terminus to generate pF-ZNF216. Zinc finger-deleted mutants, ZNF216ΔN (amino acids 36–213) and ZNF216ΔC (amino acids 1–153), were also generated by PCR and subcloned into the vectors. All cDNAs and constructs amplified by PCR were fully sequenced (ABI PRISM^{TM} 3100 Genetic Analyzer, Applied Biosystems, Foster City, CA, USA).

Northern Blot Analysis

Total RNA was denatured by glyoxal/dimethylsulfoxide and electrophoresed on a 0.9% agarose gel and transferred to a nylon membrane (Amersham Biosciences, Little Chalfont, Buckinghamshire, England). To detect the indicated mRNA, cDNA was labeled with ^{32}P with use of DNA labeling beads (Amersham Biosciences).

Immunoblot Analysis

For chasing IκBα degradation, cells were lyzed in lysis buffer (50 mM Tris-HCl, 150 mM NaCl, 1.0% NP-40, 0.5% sodium deoxycholate, 0.1% SDS, pH7.5). Aliquots of lysates were separated by SDS-PAGE and immunoblotted. Visualization was done by ECL Plus reagents (Amersham Biosciences). For nuclear translocation of NF-κB, cells were lyzed and suspended in hypotonic buffer (50 mM HEPES-KOH, 10 mM KCl, 0.1 mM EDTA, 0.1% NP-40, and protease inhibitor cocktail, pH7.8). Nuclei were pelleted by centrifugation, and the cytosolic fraction was removed. The nuclei were resuspended in extraction buffer (50 mM HEPES-KOH, 420 mM KCl, 0.1 mM EDTA, 5 mM $MgCl_2$, 2% glycerol, and protease inhibitor cocktail, pH7.8), and rotated for 30 min in 4°C. The samples were centrifuged to remove debris. Protein content was measured by using BCA protein assay reagent (PIERCE, Rockford, IL, USA).

Electrophoretic Mobility Shift Assay (EMSA)

EMSA was performed as described by Yousef with minor modification (19). Briefly, RANK293 cells treated with RANKL were washed with ice-cold PBS, and then nuclear extracts were prepared as described above. Ten micrograms of the nuclear extract were incubated with an end-labeled double-stranded oligonucleotide probe containing the sequence 5′-AAA CAG GGG GCT TTC CCT CCT C-3′ derived from the κB3 site of the TNF promoter. The reaction was performed in a total of 20 μL of binding buffer (10 mM HEPES-KOH, 50 mM KCl, 1 mM EDTA, 5 mM $MgCl_2$, 3 μg poly dI-dC, and 10% glycerol, pH7.8) for 30 min at room temperature. Samples were then fractionated in a 4% polyacrylamide gel and visualized by exposing the dried gel to film.

Reporter Gene Assay

HEK293 cells were seeded onto 24-well culture plates and transfected with 10 ng pNF-κB-Luc plasmid (Stratagene, La Jolla, CA, USA), and 5 or 25 ng of ZNF216 full-length or mutant-expressing plasmid. Twenty-four hours after transfection, cells were incubated with low-serum-containing medium (0.5% FBS) for 24 hr, and then TNFα (100 ng/mL) was added. 24 hr after the addition of the cytokine, cells were harvested. For AP-1 reporter gene assays, 100 ng

pAP1-Luc plasmid (Stratagene) was transfected with or without 250 ng ZNF216 full-length-expressing plasmid. AP-1 activation was conducted by using 10 ng pFC-MEKK positive control plasmid (Stratagene). In all transfection experiments, 10 ng Renilla luciferase expression vector, phRG-TK (Promega, Madison, WI, USA), was used as an internal control and for normalization of transfection efficiency. The luciferase activity was measured by using the Dual-Luciferase Reporter Assay System (Promega).

RESULTS

Gene Expression Profile of RANKL-Induced Osteoclast Differentiation

RANKL-treated RAW264.7 cells were efficiently differentiated to osteoclast-like cells (OCLs) within 4 days, as evidenced by multiple nuclei and expression of the osteoclast marker, TRAP (not shown). Isolated RNAs were applied to a cDNA microarray to determine the relative expression levels of about 10,000 mouse genes in response to RANKL stimulation. Analyses revealed that 208 genes were up-regulated, and 515 genes were down-regulated, more than 1.7-fold for at least one time point over a 72-h time-course. A select list of genes differentially expressed are listed in Tables 1 and 2. Genes characteristic for osteoclasts, such as vacuolar ATPases, carbonic anhydrases, and matrix metalloproteinase 9, were up-regulated (Table 1), whereas macrophage-related genes, such as lysozyme and macrophage expressed gene 1, were prominently down-regulated (Table 2). These data collectively suggest that the profiling represents the transition of macrophages into osteoclasts. Among the up-regulated genes, those encoding transcription factors were evident, including c-myc and NFATc1. It was previously reported that c-myc was strongly induced by RANKL and that a dominant negative form of c-myc suppressed osteoclast differentiation (20), suggesting c-myc as a transcription factor involved in the promotion of osteoclastogenesis under the RANKL-RANK pathway. NFATc1 was also shown to be a downstream gene of c-fos, which is known to be activated by RANKL, and osteoclastogenesis of precursor cells of c-Fos$^{-/-}$ mice was rescued by forced expression of the active form of NFATc1 (21).

Another interesting finding was the down-regulation of interferon-induced genes. Takayanagi et al. (22) showed that IFNγ was a potent inhibitor of osteoclastogenesis. Treatment of RAW264.7 cells with IFNγ resulted in rapid degradation of the adaptor protein, TRAF6, via the ubiquitin-proteasome system. The expression of STAT1, which is activated by IFNγ, was also suppressed by RANKL. These results suggest that interferon itself or a pivotal transcription factor for interferon signaling, such as STAT1, is down-regulated during RANKL-induced osteoclastogenesis.

Table 1: Genes up-regulated during RANKL-induced osteoclast differentiation. Fold increase compared to $t = 0$ at the indicated time points is shown.

Gene description	UniGene ID	Fold		
		24 hr	48 hr	72 hr
Bone resorption				
Vocuolar ATPase catalytic subunit A	Mm.29771		1.9	2.4
ATPase-like vacuolar proton channel	Mm.30155	1.7	2.1	2.5
Carbonic anhydrase 1	Mm.3471		1.9	
Carbonic anhydrase 2	Mm.1186	1.5	1.7	2.3
Matrix metalloproteinase 9	Mm.4406		2.0	1.5
Signaling				
TRAF1	Mm.12898		2.5	1.6
TRAF5	Mm.196445		2.0	
skp2	Mm.35584		3.0	1.4
Transcription				
NFATc1	Mm.329560		3.2	1.8
Myc	Mm.2444	3.1	2.1	1.5
Fra2	Mm.24684	3.7	2.7	2.6
forkhead box G1	Mm.4704		3.2	
NF-kB2	Mm.102365	2.3		
Gbx2	Mm.204730		1.9	
Hoxa2	Mm.131		2.6	
Cytokine				
IL-15	Mm.4392		2.0	1.4
PDGF	Mm.2675		2.4	
Small inducible cytokine A9	Mm.2271		2.7	2.1
Other				
Aldose reductase	Mm.451			2.7
Butyrate response factor 1	Mm.18571	1.9	1.7	1.7
DNA polymerase epsilon, subunit 2	Mm.9199		3.0	
GABA-A transporter 2	Mm.22562	1.3	1.7	2.0
H1-0 histone	Mm.24350		2.5	
gly96	Mm.25613		2.2	2.2
slug	Mm.4272		2.7	
ZNF216	Mm.292405		3.0	2.2

Expression of ZNF216 in RANKL-Induced Osteoclast Differentiation

Microarray results also indicated that the gene encoding ZNF216 was potently induced by RANKL. Although *znf216* was first identified as a candidate gene that might be involved in autosomal recessive nonsyndromic hearing loss (ARNSHL), neither disease-causing mutations nor abnormal expression of the gene was found (23). To verify the cDNA microarray results, we carried out Northern blot analysis. The entire coding region of ZNF216 was used as a probe recognizing 2.4-kb and 1.5-kb mRNA species, derived from alternative splicing and polyadenylation. Both species were up-regulated by RANKL as early as 1 hr and peaked 48 hr after addition of the cytokine (Fig. 1A). As shown in Figure 1B, induction of the protein was confirmed by immunoblotting using anti-ZNF216 antibody. An approximately 32-kDa protein was recognized and increased dramatically after RANKL stimulation. Although the expression

Table 2: Genes down-regulated during RANKL-induced osteoclast differentiation. Fold decrease compared to $t = 0$ at the indicated time points is shown.

Gene description	UniGene ID	Fold		
		24 hr	48 hr	72 hr
Macrophage-related				
Lysozyme	Mm.45436		−29.6	−11.4
Macrophage expressed gene 1	Mm.3999	−4.6	−3.3	−3.9
β2 microglobuline	Mm.163		−2.4	−2.7
Fc receptor IgE	Mm.22673		−2.5	−1.8
Fc receptor IgG high affinity I	Mm.150		−3.4	−2.8
Histocompatibility 2 L region	Mm.260691		−1.9	−1.4
Histocompatibility 2 Q region	Mm.34421		2.4	−2.1
Histocompatibility 2 T region	Mm.221296		−2.2	−2.3
Signaling				
Adenylate cyclase 7	Mm.288206	−1.3	−2.0	−1.6
Adenylate cyclase-associated CAP protein	Mm.8687		−3.5	−3.0
Calmodulin 2	Mm.18041		−1.9	−1.5
STAT 1	Mm.8249		−2.2	−2.3
JAK2	Mm.809	−2.2		
Ribosomal protein S6 kinase, polypeptide 4	Mm.20914		−2.1	
MAPK14	Mm.4437		−1.7	−2.2
MAPKKK1	Mm.15918		−2.0	−1.5
AMP-dependent protein kinase	Mm.16766	−1.7	−1.9	−2.1
fyn proto-oncogene	Mm.4848		−1.6	−2.0
Cell cycle and differentiation				
Id2	Mm.34871		−3.8	−2.2
Id3	Mm.110		−2.0	−2.5
cyclin D1	Mm.273049		−1.6	−2.3
cdk2	Mm.118			−2.0
p21	Mm.34446	−1.3	−1.7	−2.5
Matrix protein and secreted-protein related				
ADAM15	Mm.19830		−1.9	−2.0
ADAM17	Mm.355306		−2.2	−1.8
IGF-1	Mm.268521	−3.6	−2.2	
IGF-1 binding protein 4	Mm.233799		−2.2	−2.3
Osteopontin	Mm.288474	−2.6	−4.0	−1.6
Interferon induced gene				
Interferon activated gene 203	Mm.261270	−2.2	−2.1	−2.0
Interferon activated gene 204	Mm.212870		−2.5	
Interferon dependent positive acting transcriptio factor 3	Mm.2032		−1.8	−2.0
Interferon γ inducible protein	Mm.24769		−2.0	−1.5
Interferon regulatory factor 5	Mm.6479		−2.0	−2.0
Interferon regulatory factor 7	Mm.3233		−3.8	−3.0
Interferon induced protein with tetratricopeptide repeat 3	Mm.271850		−1.5	−2.4
2′-5′ oligoadenylate synthetase 1A	Mm.14301	−1.5	−3.6	−1.4
Lysosomal protein				
Cathepsin D	Mm.231395		−3.0	−2.3
Cathepsin L	Mm.930	−1.5	−4.8	−5.9
Cathepsin S	Mm.3619	−2.4	−2.6	−2.1
Lysosomal membrane glycoprotein 2	Mm.486		−2.4	−1.7
Other				
Annexin A2	Mm.238343		−1.6	−2.1
Caspase 1	Mm.1051	−1.7	−1.5	−2.6
Coronin	Mm.27317	−1.7	−2.4	−2.1
Amyloid beta precursor protein	Mm.277585	−1.5	−1.8	−2.1
Glycoprotein 49A	Mm.196617			−2.6
Glycoprotein 49B	Mm.34408	−3.2	−4.0	−2.2
LIM only 2	Mm.29266		−2.9	−3.2
Schlafen 4	Mm.38192	−1.6	−5.1	−2.4
Cell surface glycoprotein EMR 1 precursor	Mm.258979	−2.5	−3.1	−3.5
Peroxiredoxin 4	Mm.247542			−1.9
Peroxiredoxin 5	Mm.279782			−2.1
Pleckstrin	Mm.98232		−6.6	−2.3

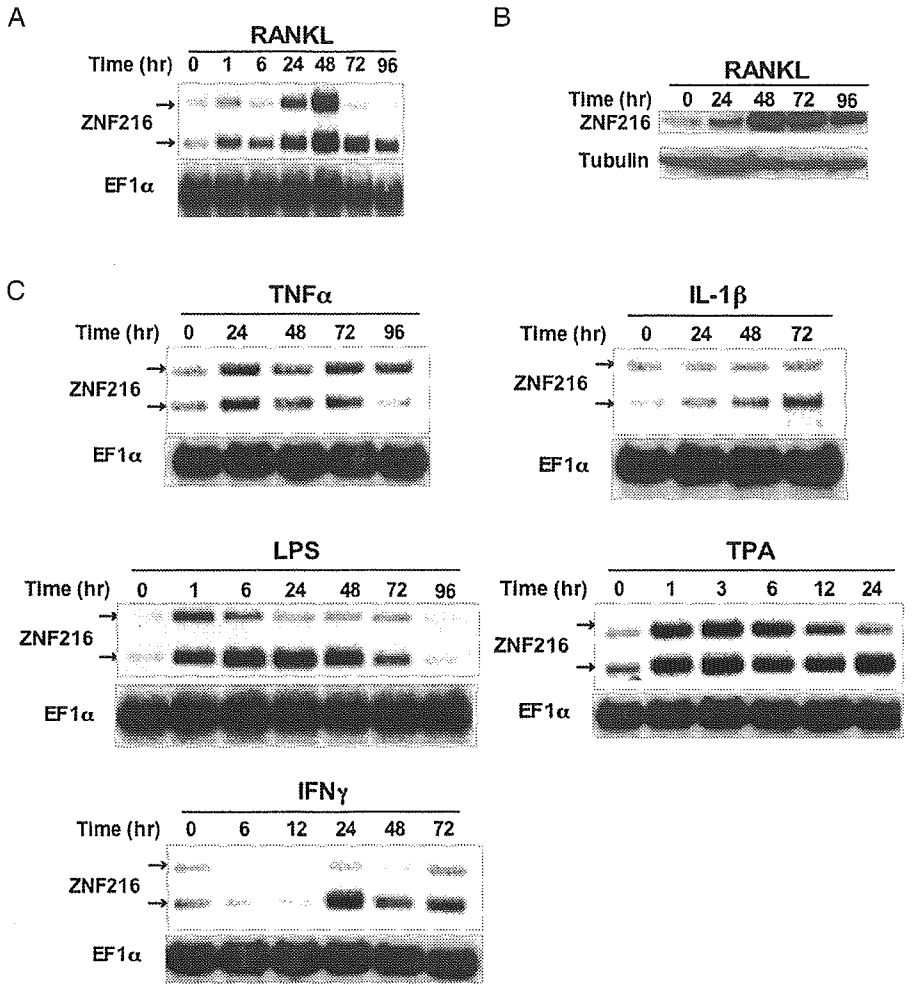

Figure 1: Expression of ZNF216. (A) The expression of ZNF216 is induced by RANKL. RAW264.7 cells were treated with RANKL (10 ng/mL) for the indicated time, and purified RNA was subjected to Northern blot analysis. The same membranes were reprobed for EF1α (elongation factor 1α) to control for loading. (B) Immunoblot analysis. The induction of ZNF216 protein is shown throughout a 96-hr time-course. The membrane was reprobed with tubulin antibody to control for protein loading. (C) Other proinflammatory cytokines or stimulators also induced ZNF216. Total RNA was prepared at the indicated time and probed for ZNF216 mRNA expression. The membrane was reprobed for EF1α as described above to control for loading.

pattern of the protein was well concordant with that of the RNA, the peak level of ZNF216 protein persisted long after 72 hr, when the RNA level had subsequently declined. RANKL-induced expression of ZNF216 was also observed in primary cultures of bone marrow macrophages (data not shown).

To examine whether expression of ZNF216 could be induced by other TNF superfamily cytokines, RAW264.7 cells were treated with TNFα. As expected,

TNFα up-regulated ZNF216, although not as much as RANKL (Fig. 1C). Both RANKL and TNFα activate a common signaling pathway through NF-κB and JNK with TNFR-associated factor (TRAF) family members (24). This intracellular pathway is known to be partially shared by those of IL-1β and LPS. As shown in Figure 1C, the expression of ZNF216 was also increased by treatment with both IL-1β and LPS. It is of interest that the expression was rapidly induced by LPS within 1 hr (Fig. 1C). In contrast, ZNF216 expression induced by IL-1β was rather weak. Thus, we hypothesized that activators of NF-κB or AP-1 might also induce ZNF216 expression. TPA, a potent activator of protein kinase C (PKC), activates NF-κB and AP-1 in rat 3Y1 fibroblasts and in the human gastric cancer cell line, MGC80-3 (25–27). As shown in Figure 1C, expression of ZNF216 was strongly induced by TPA in RAW264.7 cells. In addition, the antiviral cytokine, IFNγ, which is not known as an activator of NF-κB or AP-1, also up-regulated the expression of ZNF216 (Fig. 1C).

Ectopic Expression of ZNF216 in Osteoclast Differentiation

The ZNF216 protein is composed of 213 amino acid and contains both A20-like and AN1-like zinc finger domains (Fig. 2A). The A20-like zinc finger domain is a C2/C2 type zinc finger localized between amino acids 11–35 at the N-terminus (Fig. 2A). The AN1-like zinc finger domain is localized at amino acids 154–193 and contains the sequence CX2CX(9–12)CX(1–2)CX4CX2HX5HXC, which is similar to that of AN1, a ubiquitin-like protein in Xenopus laevis (28). To clarify the molecular function of ZNF216 in osteoclast differentiation, we generated RAW264.7 cells stably expressing either full-length or truncated forms of ZNF216, and in vitro osteoclastogenesis assays were performed. Comparable expression of ZNF216 and its mutants were confirmed by immunoblot analyses (Fig. 2A, right panel). Proliferation was not significantly affected by ectopic expression of ZNF216 mutants (not shown). Stably transfected RAW264.7 cells were seeded in 96-well plates and stimulated with RANKL for 48 hr. It is surprising that ectopic expression of full-length ZNF216 significantly suppressed TRAP-positive cell number compared with mock-infected RAW264.7 cells (Figs. 2B and C). By contrast, RAW cells expressing deletion mutations in either zinc finger domain (ΔN or ΔC) exhibited accelerated osteoclast differentiation monitored by TRAP (Figs. 2B and C). In particular, the C-terminal zinc finger domain truncated mutant (ΔC) dramatically promoted the expression of TRAP. Most of RAW264.7 cells expressing ΔC mutant were positive for TRAP, whereas mock-infected cells were only 25% TRAP positive (Figs. 2B and C). Ectopic expression of truncated mutants in RAW264.7 cells did not possess any TRAP activity without RANKL treatment, indicating that RANKL was required for the observed effects of on osteoclast differentiation (data not shown).

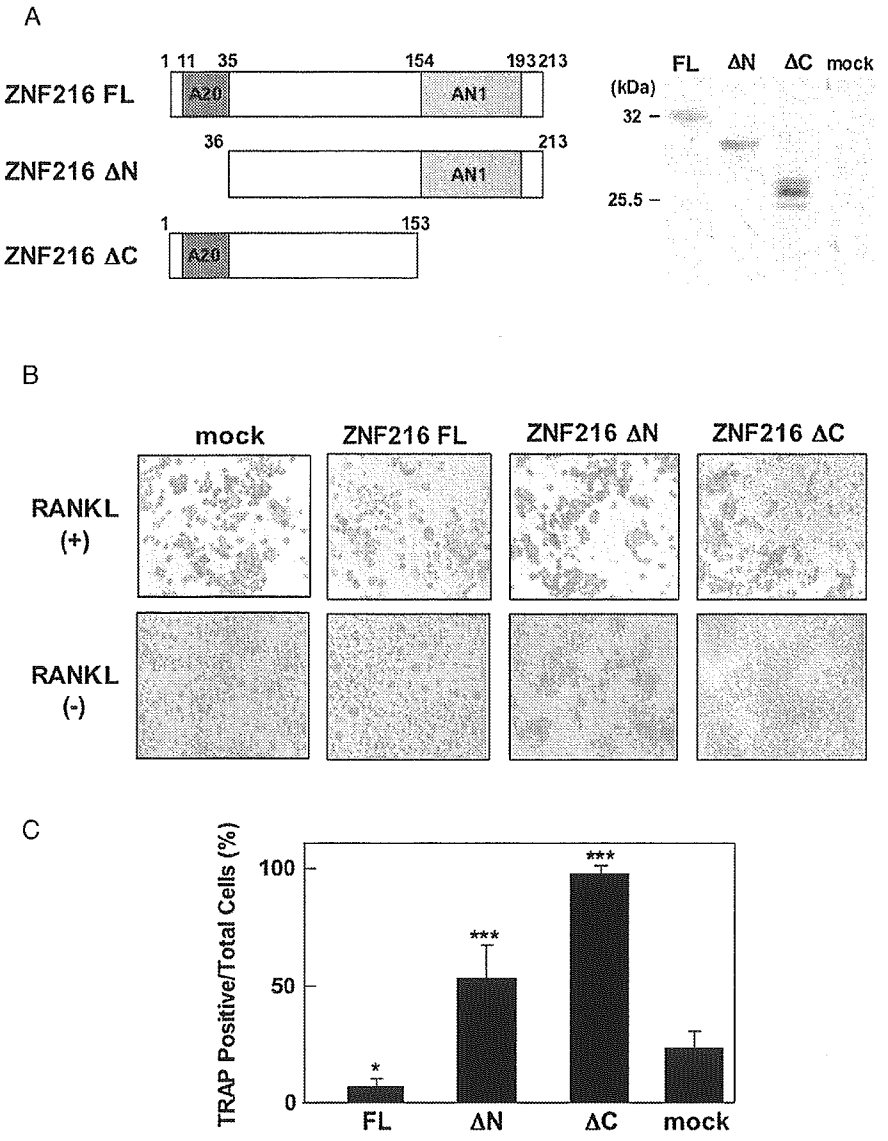

Figure 2: ZNF216 inhibits osteoclastogenesis. (A) Schematic presentation of ZNF216 and its deletion mutants (left panel). Full-length ZNF216 (213 amino acids) is denoted as ZNF216-FL. A20-like (*dark gray box*) or AN1-like (*gray box*) zinc finger domains were deleted in ZNF216-ΔN or ZNF216-ΔC, respectively. The number represents the positions of the deleted amino acid residues. Expression of ZNF216 and its mutants in RAW264.7 cells (right panel). The expression levels of the proteins in stable transfectants were comparable. ZNF216 proteins were detected by immunoblotting with anti-FLAG antibody. (B) Ectopic expression of ZNF216 inhibits RANKL-mediated osteoclastogenesis in RAW264.7 cells. Three individual RAW264.7 cell clones stably expressing full-length or truncated forms of the zinc finger domains were seeded and treated with (upper panels) or without (lower panels) RANKL (10 ng/mL). After 48 hr, cells were fixed and TRAP activity was determined. No TRAP-positive cells were observed in all cell lines without RANKL treatment. (C) The number of TRAP-positive (purple) cells, in (B), were quantified. Results represent the average values from the three clones. $^{*}P < 0.05$ vs. mock-infected cells; $^{***}P < 0.005$ vs. mock-infected cells.

ZNF216 in the NF-κB Signaling Pathway

The inhibitory effects of ZNF216 we observed, along with a recent report indicating that ZNF216 inhibits NF-κB activation (29), prompted us to investigate the relationship between ZNF216 and NF-κB signaling in osteoclastogenesis. For NF-κB activation, the degradation of its inhibitory binding molecule, IκB, is crucial. Activation of the NF-κB pathway requires phosphorylation of IκB leading to its degradation via the ubiquitin-proteasome system (30). As shown in Figure 3A, IκBα was rapidly degraded by LPS in mock-transfected RAW264.7 cells. Neither the full-length nor the truncated mutants of ZNF216 affected IκBα degradation (Fig. 3A). NF-κB dissociated from IκB exposes its nuclear localization signal. Thus, we investigated cytoplasmic to nuclear translocation of NF-κB in RANK293 cells, which are a cell line derived from HEK293 cell stably transfected with a vector to express RANK. Cells were treated with RANKL, and the nuclear fraction subsequently extracted and monitored for the translocation of NF-κB. As shown in Figure 3B, there were no significant alterations in the nuclear translocation of p50, p52, and p60 NF-κB subunits between mock- and ZNF216-infected cells. ZNF216 was localized predominantly in the cytoplasm and to a lesser extent in the nucleus (data not shown). We next examined whether ectopic expression of ZNF216 disrupted the binding ability of NF-κB to its target promoter. Although no band shift was observed in nuclear extracts from nontreated RANK293 cells, RANKL-treated cell extracts showed a prominent band shift (Fig. 3C). The binding ability of NF-κB to oligo probe was not affected by expression of either full-length or truncated mutants of ZNF216 (Fig. 3C). Finally, neither the expression of full-length nor truncated mutants of ZNF216 affected transcription of the reporter luciferase gene driven by the NF-κB promoter after TNFα stimulation (Fig. 3D) or the AP-1 promoter (Fig. 3E). Together, these results suggest that ZNF216 is not directly involved in the NF-κB signaling pathway.

DISCUSSION

In the present study, we have identified genes regulated in RANKL-induced osteoclast differentiation. Although some of the up-regulated genes have been previously reported to be involved in osteoclast differentiation, the majority of the down-regulated genes have not been described. Recently, it was demonstrated that the ITAM-bearing protein family of transmembrane adaptors, such as DAP12, play critical roles in osteoclast development and function (31–33). These co-stimulatory adaptors are known to be associated with Fc receptors in the modulation of their signals (34,35). Notably, the expression of Fc receptors were down-regulated during osteoclast differentiation in our study (Table 2), suggesting that the function of the ITAMs may not associated with the Fc receptors, but other cell surface molecules, such as TREM2 (36,37).

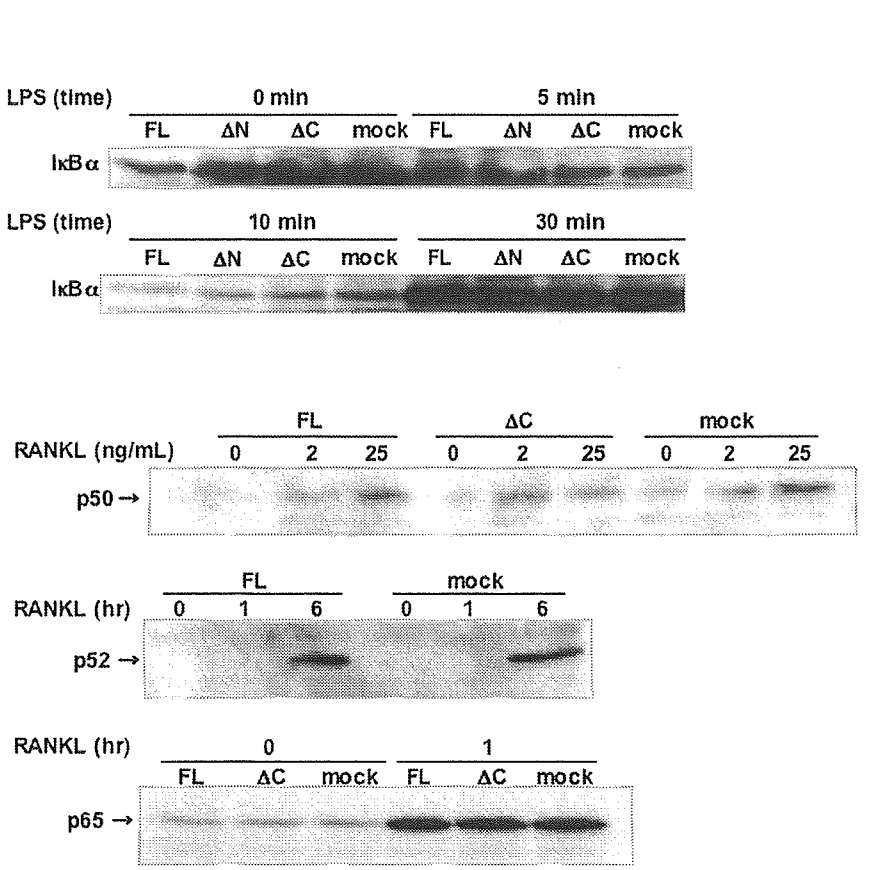

Figure 3: ZNF216 does not inhibit the NF-κB pathway. (A) Degradation of IκBα protein by LPS. RAW264.7 cells stably expressing the indicated constructs were stimulated with 10 μg/mL LPS. At the indicated time points, cells were lysed and analyzed for IκBα protein by immunoblotting. (B) Expression levels of the NF-κB protein subunits. RANK293 cells were transfected with the indicated vector constructs. Cells were then treated with 0, 2, and 25 ng/mL RANKL for 30 min. Nuclear fraction was isolated and subjected to immunoblot analysis for the p50, p52, and p65 NF-κB subunits. Cells were treated with 10 ng/mL RANKL for the indicated time periods, and immunoblot analyses were performed. (C) RANKL-dependent band shift of NF-κB. EMSA analyses were conducted with nuclear extracts from the indicated vector constructs in RANK293 cells as described in Materials and Methods. Arrow indicates nonbound free probe. (D) TNFα-dependent NF-κB reporter gene activation. HEK293 cells were transfected with 5 ng or 25 ng of the indicated ZNF216 constructs and 10 ng of pNF-κB-Luc. All luciferase activities were corrected with renilla luciferase activities. Each experiment was performed at least in triplicate, and data are expressed as the means ± SD. (E) Effect on AP-1-dependent transcription. HEK293 cells were transfected with 10 ng MEKK-expressing plasmid and 250 ng ZNF216 full-length plasmid. All luciferase activities were corrected with renilla luciferase activities. Each experiment was performed at least in duplicate, and data are expressed as the means ± SD. *(Continued)*

Interferons have also been shown to play important roles in physiological and pathological osteoclast function (38). IFNβ is induced by the RANKL-RANK pathway through Fos and inhibits the function of the transcription factor, forming a negative feedback loop (39). In our studies, significant decreases in

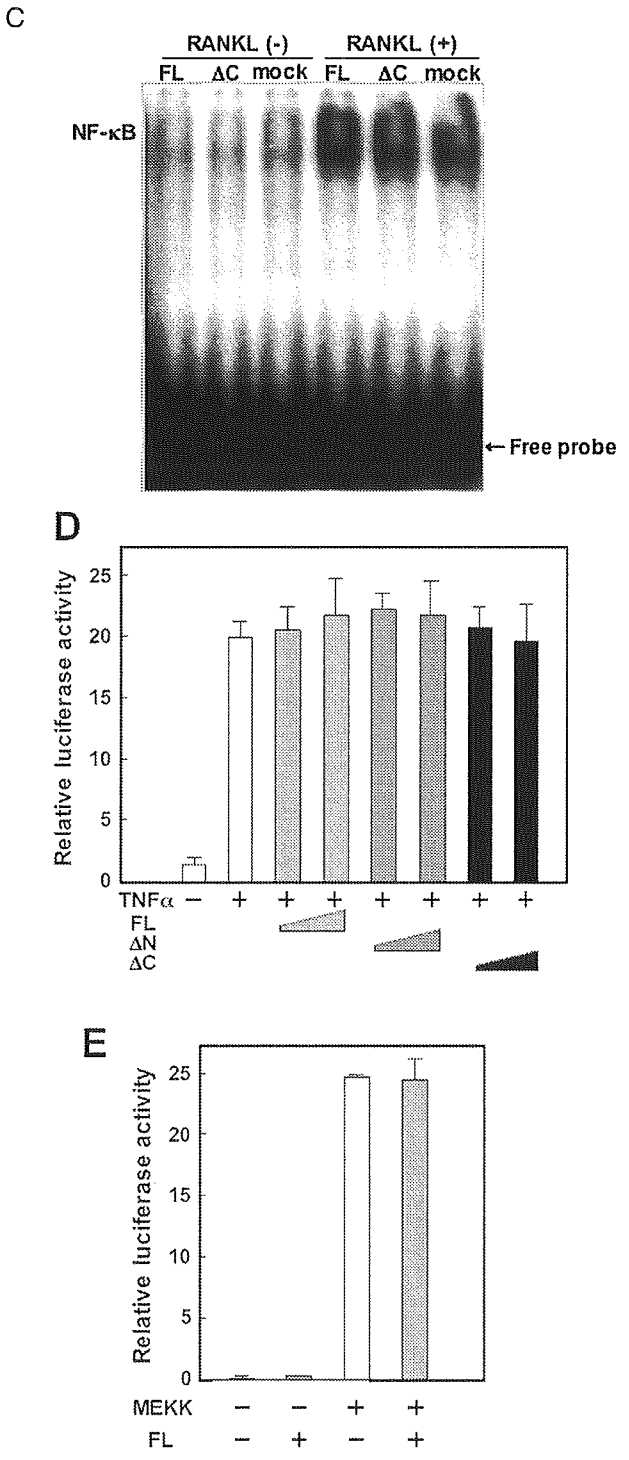

Figure 3: (Continued)